Antarctic Science 28(4), 277–292 (2016) © Antarctic Science Ltd 2016 doi:10.1017/S0954102015000681

Determination of an experimental geoid at Deception Island, South Shetland Islands, Antarctica

BISMARCK JIGENA[1,2], MANUEL BERROCOSO[2,3], CRISTINA TORRECILLAS[2,4], JUAN VIDAL[2,5], IGNACIO BARBERO[5] and ALBERTO FERNANDEZ-ROS[2,3]

[1]*Department of Nautical Sciences and Maritime Studies, University of Cádiz, CP 11510, Puerto Real, Cádiz, Spain*
[2]*Astronomy, Geodesy and Cartography Laboratory (LAGC-UCA), University of Cádiz, Faculty of Science, CP 11510, Puerto Real, Cádiz, Spain*
[3]*Department of Mathematics, University of Cádiz, CP 11510, Puerto Real, Cádiz, Spain*
[4]*Department of Graphic Engineering, University of Seville, CP 41092, Seville, Spain*
[5]*Department of Naval Construction, University of Cádiz, CP 11510, Puerto Real, Cádiz, Spain*
bismarck.jigena@gm.uca.es

Abstract: Deception Island is an active volcano located in Bransfield Strait. Its volcanic activity is linked to the presence of gravity anomalies that influence the definition of the geoid. In this paper, a precise undulation geoid model (GeoiDEC14) has been computed from GPS, gravimetric and levelling measurements. GeoiDEC14 highlights local anomalies of the island that match with hot spots, such as the minimum values shown in Fumarole Bay and Whalers Bay (fumarole areas), or the maximum values found in the remains of lava at Colatinas, Black Glacier and Murature Point. Comparison of GeoiDEC14 with global models always shows negative values due to an average of 18.80 m for our model compared to 19.80–20.60 m for models such as ITSG-Grace2014s, EGM08, AIUG-Grace03s or EGM96. This difference is due to the lack of resolution of global models and to the volcanic activity on the island. To confirm the results, the same measurements were taken on nearby Livingston Island. The values of geoid undulation on this island reaffirm the lack of detail in the global geoid in the area, presenting an average of 18.90 m, similar to the average value of GeoiDEC14.

Received 15 January 2015, accepted 3 November 2015, first published online 24 February 2016

Key words: geoid undulation, gravimetric, levelling, Livingston Island, mean sea level, orthometric height

Introduction

The geoid is a vertical reference system. It can be obtained by combining GPS and gravimetric observations with orthometric heights. The evaluation of the volcanic surface deformation parameters is made by analysing the horizontal and vertical deformation models obtained from GPS observations. However, the lack of physical meaning of the ellipsoidal height makes it necessary to establish a physical and mathematical reference framework, in this case the geoid, in order to calculate accurate vertical deformations. The geoid, together with digital elevation models, constitute the main reference system for designing models of lava flow to determine a hazard map and identify risk areas in advance.

The Spanish and Argentinean bases on Deception Island have contributed to research groups. These countries have systematically conducted monitoring of the volcanic and tectonic activities on Livingston and Deception islands (South Shetland Islands, Fig. 1). In 1988, the first stations of the Red Geodésica de Isla Decepción (REGID) geodetic network were established in order to study the geodynamic activity on the Deception volcano and its environment (Berrocoso *et al.* 2006; Fig. 2). This monitoring detected two important volcanic crisis on active Deception Island in December and January 1991, and in January and February 1999.

In 1992, a topographical map was produced of Deception Island establishing an initial geoid undulation (N) value of -13.00 m (CGE 1992). The first experimental geoid for Deception Island, included in the Multidisciplinary Scientific Information Support System (SIMAC) for Deception Island (Torrecillas *et al.* 2006, Berrocoso *et al.* 2008), was calculated according to this elevation reference for the BARG geodetic benchmark (Fig. 3), providing a mean N value of -19.59 m in that area in 2008 (Berrocoso *et al.* 2008, 2012). This value differed from the 1992 value by 6.59 m.

The first sea level observations at Deception Island were made by the Argentine Naval Hydrographic Survey (Servicio de Hidrografía Naval) in 1970. Tidal data were obtained over five days in summer, by means of a visual tide staff located close to the BARG geodetic benchmark at the Argentinean Deception Station. During the 2001–02 and 2002–03 Spanish Antarctic campaigns, the Red de Nivelación de Isla Decepción (RENID) levelling network was established determining the first vertical datum for Deception Island, taking the BARG geodetic benchmark

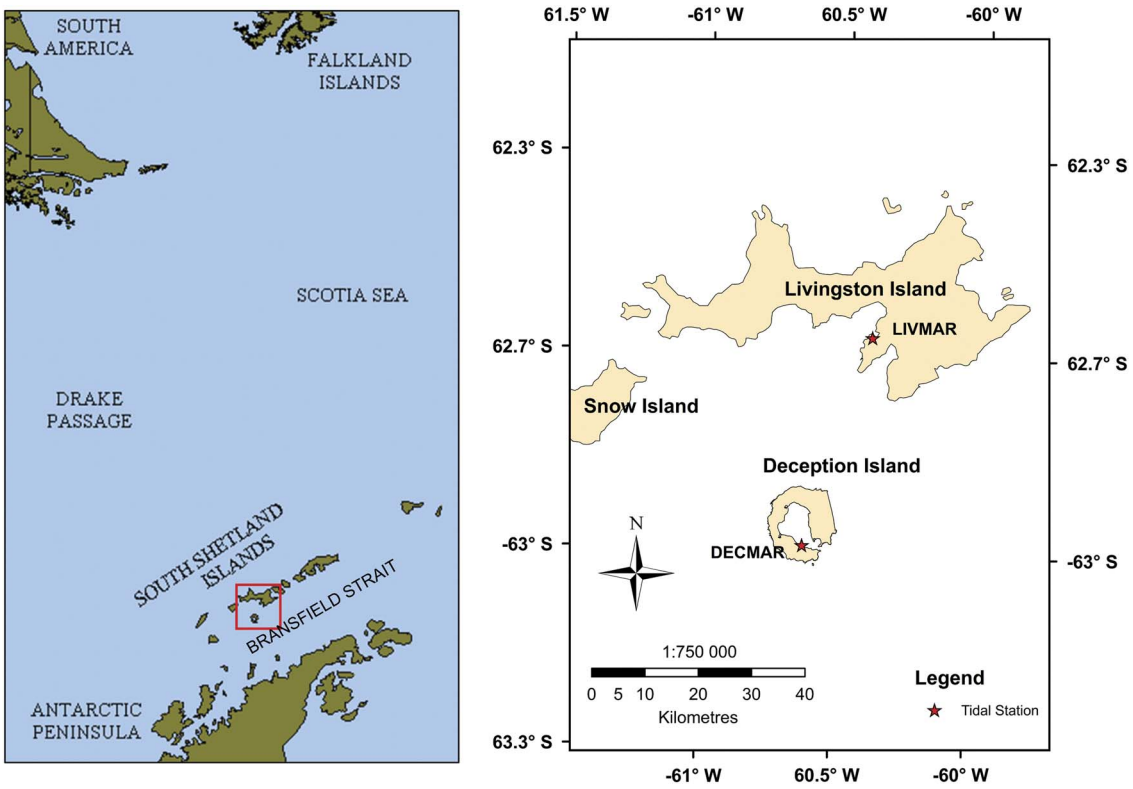

Fig. 1. Maps showing **a.** the study area (red polygon) and **b.** Livingston and Deception islands. The red stars indicate the locations of the DECMAR and LIVMAR tidal gauge stations.

as a fundamental levelling point, with an orthometric height value of 2.55 m above mean sea level (a.m.s.l.). This orthometric level was translated by geometric levelling to the LN00, the new fundamental levelling point of the RENID network, with a value of 5.43 m a.m.s.l. (Fig. 4). From this vertical datum, levelling elevations were given at all points of the RENID network (Berrocoso *et al.* 2008). Gravimetric observations were carried out at these points and at other locations around Port Foster, with a total of 108 gravimetric points, in order to establish the Red Gravimétrica de Isla Decepción (REGRID) gravimetric network (Fig. 5). These were not the first gravimetric measures carried out on the Island, as previous readings were carried out in the summer of 1999/2000 (Carbó *et al.* 2001), as a response to the seismic crisis in 1999.

Since 2007, the Laboratory of Astronomy, Geodesy and Cartography of the University of Cádiz (LAGC-UCA) has been carrying out new geometric levelling, trigonometric linkages, GPS observations and observations of tidal data on Livingston and Deception islands. During the 2007–08 Spanish Antarctic campaign, two tidal gauges were installed in order to obtain the first tidal constituents and mean sea level for Livingston and Deception islands. The first, LIVMAR, was installed on Livingston Island at Johnsons Dock, near the BEJC geodetic point (Fig. 1), and the second, DECMAR, on Deception Island at Colatinas Point.

In 2011, the first results of direct observations of mean sea level were obtained (Vidal *et al.* 2012). Subsequently, better results have been obtained in the determination of the mean sea level in Livingston and Deception islands, making a new adjustment with a two-year time series and calculating a new control value of the orthometric height for LN00 geodetic benchmark of 6.20 m a.m.s.l. (Jigena *et al.* 2014). A suitable determination of the mean sea level significantly influences the determination of the geoid (Reyes *et al.* 2015). For that reason, these data have been fundamental for the accurate determination of a new local geoid for Deception Island. GeoiDEC2014 is the result of the present work, which shows an improvement relative to the results obtained in 2008.

Regional setting

Deception and Livingston islands are part of the South Shetland Islands archipelago, the northernmost extremity of Antarctica (Fig. 1). Separating these islands from the Antarctic Peninsula is Bransfield Strait, which represents one of the most interesting geodynamic regions in Antarctica due to the convergence of several

https://doi.org/10.1017/S0954102015000681 Published online by Cambridge University Press

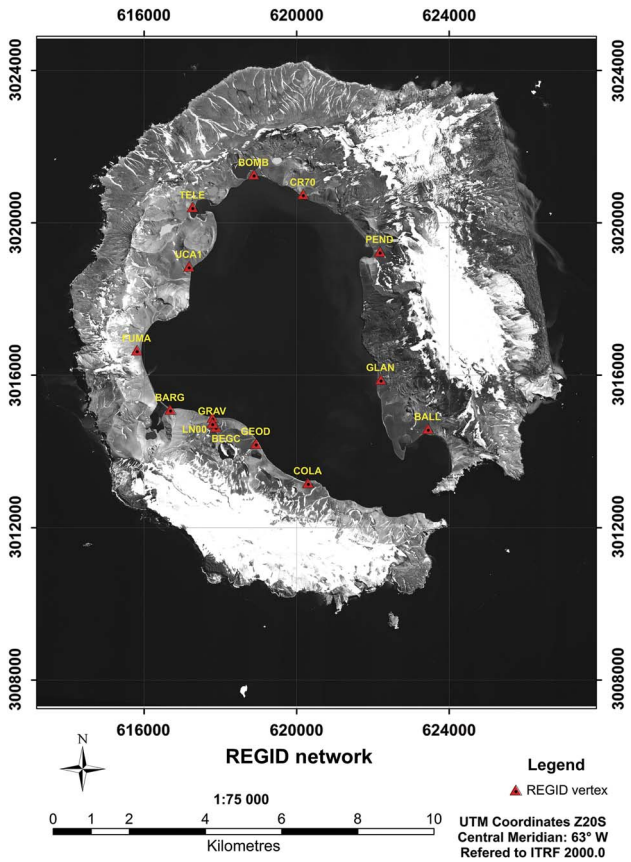

Fig. 2. The REGID network.

tectonic plates. The strait is *c*. 120 km wide and *c*. 500 km long running in a NE–SW direction between latitudes 60°S and 63°S. It is an active marginal basin occupied by six volcanic edifices aligned approximately along the main direction of the basin (Gracia *et al.* 1997). This strait is bounded to the south-east by a ridge and to the north-west by a former trench.

Deception Island is an active volcanic island younger than 0.75 Ma (Valencio *et al.* 1979). The volcanic sequence that built up Deception Island evolved from submarine pillow lavas to subaerial eruptions, mainly Strombolian and phreatomagmatic (Martí *et al.* 1996, Smellie 2001, Smellie *et al.* 2002, Maestro *et al.* 2007). The island evolved through the collapse of a huge volcanic edifice under a regional stress. The present landscape shows a horseshoe-shaped island with a flooded, well-developed, collapsed caldera of 9–10 km diameter called Port Foster (Fig. 6). Port Foster opens onto Bransfield Strait through a shallow and narrow sill called Neptunes Bellows. Historic volcanism on Deception Island principally affected the inner rim of the volcanic caldera and was associated with fractures with regional orientations NNW–SSE and NE–SW (Martí *et al.* 1996). The caldera boundary and the collapsed scarp have affected pre-caldera deposits and the location of post-caldera eruptive centres and cinder cones (Smellie 2001, 2002, Smellie *et al.* 2002). Eruptions at high elevations were Strombolian with small magma volumes. The duration of these eruptions are unknown, with some small lava flows which flowed towards Port Foster. Eruptions at lower elevations were principally phreatomagmatic and produced tuff cones and maars. Historical eruptions took place in 1839, 1842, 1912, 1917, 1967, 1969 and 1970 (Smellie *et al.* 2002; see Fig. 6).

Livingston Island is the second largest of the South Shetland Islands archipelago at *c.* 70 km long and varing from 4–32 km wide in an E–NE to W–SW direction. Livingston Island has no volcanic activity.

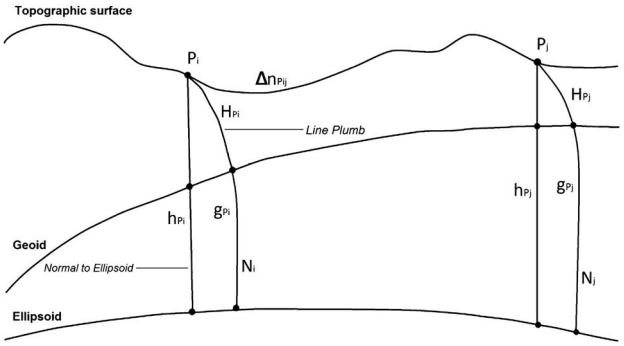

Fig. 3. Relationship between the geoid, ellipsoid and topographical surface, according to variables of Eq. (2).

Methodology

The developed method consisted of the determination of the geoid undulation (N) from the difference between ellipsoidal height (h) directly obtained by means of GPS observations and orthometric height (H), obtained by geodesic levelling (geometric or trigonometric) and corrected with gravity measurements (Heiskanen & Moritz 1967, Berrocoso *et al.* 1996). This methodology was used because it is easy to implement computationally, is quite rigorous and demanding regarding input data, and also offers the best results in areas with a radius of < 50 km (Leick 2004). As opposed to other methodologies, such as the Remove-Restore method, provided there is sufficient data densification to guarantee the quantity and quality.

Using the geometrical relationship between the geoid undulation (N), the ellipsoidal height (h) and the orthometric height (H), obtained from geometric levelling and corrected for gravimetric effects, the geoid undulations are calculated by means of the well-established formula:

$$h = H + N. \quad (1)$$

Viewing Fig. 3, considering that the study area is relatively small and starting from a point P_i with a

https://doi.org/10.1017/S0954102015000681 Published online by Cambridge University Press

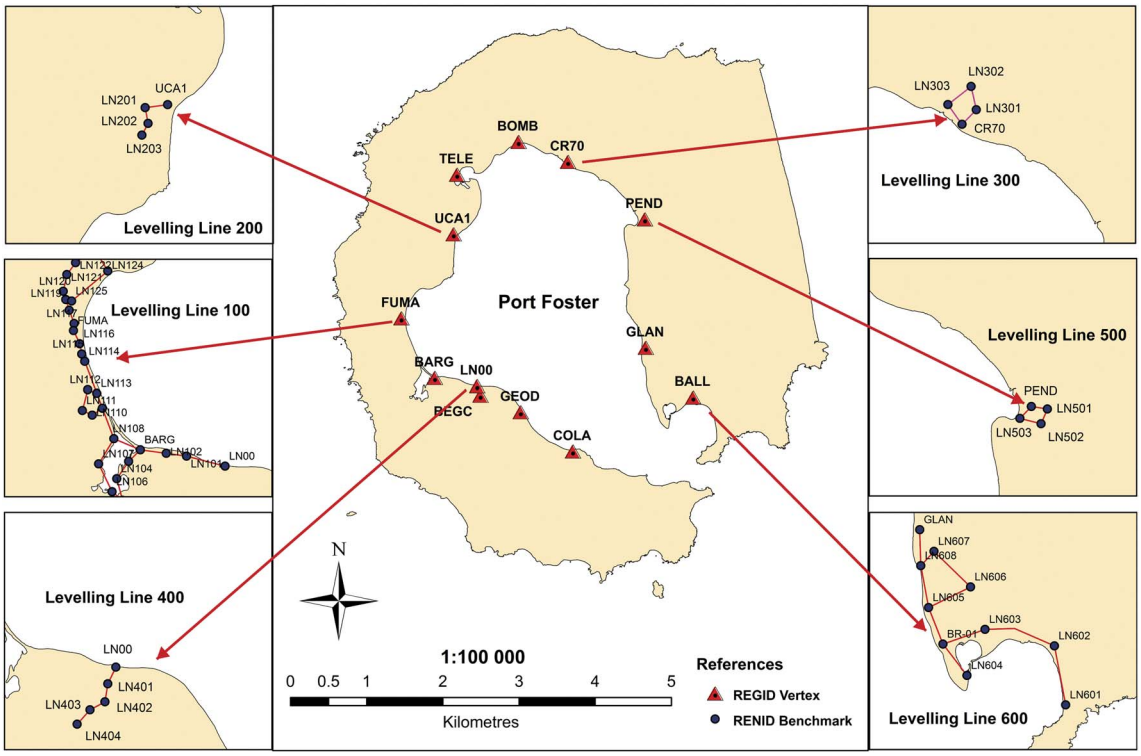

Fig. 4. The RENID levelling network.

known orthometric height (H_{Pi}), the following point P_j is considered to be sufficiently close so as to directly unite them by means of a single section of levelling; in short, to obtain the value of the orthometric height of a point P_j (H_{Pj}) knowing the orthometric height at a point P_i, the difference of level between both points, and the value of the gravity at these points, the following equation is used (Berrocoso *et al.* 1996, p. 92–93):

$$0.0424 * 10^{-3} H_{P_j}^2 + \overrightarrow{g_{P_i}} H_{P_j} - \left(\overrightarrow{g_{P_j}} \Delta n_{P_{i,j}} + \overrightarrow{g_{P_i}} H_{P_i} + 0.0424 * 10^{-3} H_{P_i}^2 \right) = 0. \quad (2)$$

The orthometric height H_{P_j} of the point P_j can be calculated from the orthometric height H_{P_i} of the reference point P_i , the geometric level difference $\Delta n_{P_{i,j}}$ between P_i and P_j and the values of the absolute gravity, $\overrightarrow{g_{P_i}}$ and $\overrightarrow{g_{P_j}}$, at these points.

Equation (2) is of the second order and provides the orthometric height of P_j. Although this equation has two solutions, only one will be a valid value, the other value will be mathematically unsound.

The following values were used in the calculation of the complete development performed to obtain Eq. (2): $\gamma_0^{45^\circ} = 980629.388$ mGal, the normal gravity value at sea level at a latitude of 45°, which is approximate for the WGS84 reference ellipsoid, $k = 6.67 \times 10^{-11}$ Nm^2 kg^{-2} in SI units, k is the gravitational constant, and $\rho = 2670$ kg m^{-3} the density of the crust.

The value used for ρ corresponds to the average value of continental crustal that was used by Carbó *et al.* (2001)

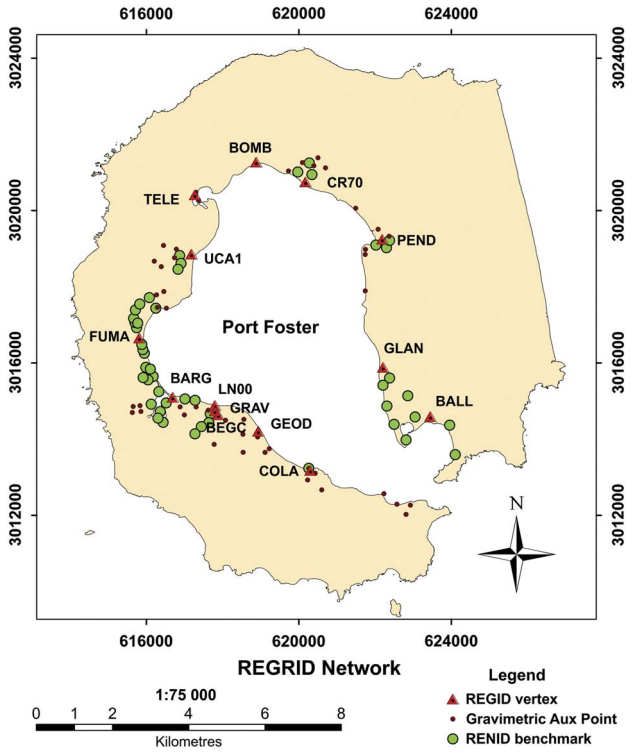

Fig. 5. The REGRID network.

https://doi.org/10.1017/S0954102015000681 Published online by Cambridge University Press

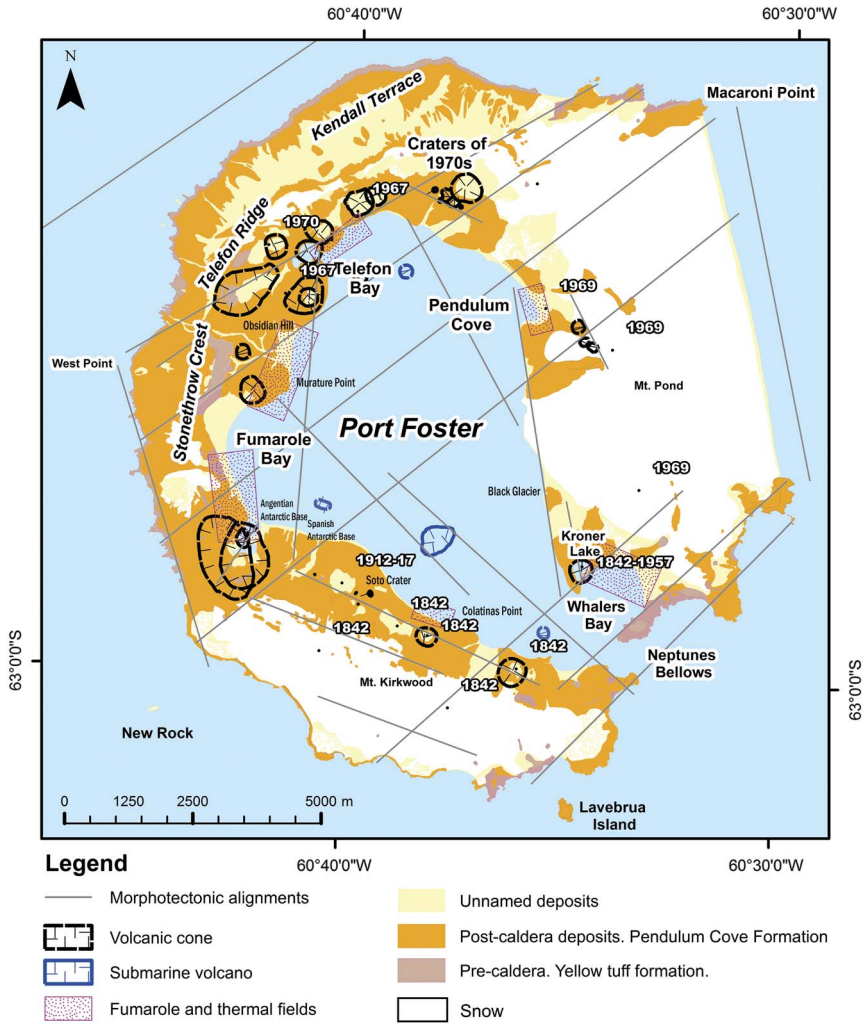

Fig. 6. Map showing the simplified geology of Deception Island (after Smellie *et al.* 2002) and the locations of historical eruptions.

for the correction of the gravimetric readings in the terrestrial part of Deception Island.

The associated errors at each point were obtained by applying the errors propagation law to the method for geoid determination, where the variance of N is equal to the sum of the variances of h and H. Thus, the total error becomes:

$$\sigma_N = \left[\sigma_h^2 + \sigma_H^2\right]^{1/2}, \tag{3}$$

where the ellipsoidal height error is obtained from the GPS data processing and the orthometric height error is calculated by means of the following expression:

$$\sigma_{H_{P_j}} = \frac{1}{R_{i,j}}\left[\left(\frac{R_{i,j} - \overrightarrow{g_{P_j}} + 0.848 \cdot 10^{-4}\Delta n_{P_{i,j}}}{0.848 \cdot 10^{-4}}\sigma_{g_{Pj}}\right)^2 + \left(\overrightarrow{g_{P_j}} \cdot \sigma_{\Delta n P_{i,j}}\right)^2 + \left(H_{P_i} \cdot \sigma_{g_{P_i}}\right)^2 + \left(\left(\overrightarrow{g_{P_i}} + 0.848 \cdot 10^{-4}\right)\sigma_{H_{P_i}}\right)^2\right]^{1/2}, \tag{4}$$

with P_i being the reference point and known orthometric height and P_j the computation point. The value of $R_{i,j}$ is equal to:

$$R_{i,j} = \left[\left(\overrightarrow{g_{P_j}}\right)^2 + 1.696 \cdot 10^{-4}\left(\left(\overrightarrow{g_{P_j}}\right)^2 \cdot \Delta n_{P_{i,j}} + g_{P_i} \cdot H_{P_i} + 0.424 \cdot 10^{-4} H_{P_i}^2\right)\right]^{1/2}. \tag{5}$$

In the calculation of errors, the error obtained in the determination of the mean sea level at both tide gauge stations was taken as follows. At Deception Island, taking into account COLA geodetic benchmark, for which the error was ± 0.051 m from DECMAR Station. This error was added to the levelling error between COLA and LN00, obtaining an initial error of 0.088 m for the benchmark LN00. All of the points of the RENID network were propagated from this vertex. In the case of Livingston Island, the error at BEJC was ± 0.084 m from LIVMAR tidal station and propagated to the other two points on this island, BEJ1 and TOJO.

https://doi.org/10.1017/S0954102015000681 Published online by Cambridge University Press

Equipment, data acquisition and data processing

In order to determine the experimental geoid, it was necessary to have a complete set of data consisting of GPS observations, levelling data and gravimetric measurements. The data used pertain to the LAGC-UCA taken during the 1989–90 to 2012–13 Spanish Antarctic campaigns. The global navigation satellite system (GNSS)-GPS gravimetric and levelling data were acquired for geodesic and geophysical purposes for the establishment of geodetic, levelling and gravimetric networks in the Antarctic, and mainly for the Deception and Livingston islands (Berrocoso *et al.* 2008). From the 2007–08 until the 2012–13 campaign, the geodetic networks were updated and extended, weather and tidal data were obtained for the determination of the mean sea level, the geodesic reference framework was updated and new cartography obtained (Torrecillas *et al.* 2011, Berrocoso *et al.* 2012, Vidal *et al.* 2012, Jigena *et al.* 2014).

The specific data that is used in the calculation of the geoid of Deception Island must comply with the technical and geodesic specifications that guarantee the quality of such, in particular: i) A geodesic and/or gravimetric network must include all of the geodesic points that were designed and established with this intention and whose data have been collected, processed and adapted under geodesic standards. This is the case for the REGID, RENID and REGRID networks (Figs 2, 4 & 5). ii) Co-ordinates must be referenced to a unique reference system with respect to International GNSS Service (IGS) stations. In our case, GPS solutions were used in ITRF2000.0 co-ordinates (Altamimi *et al.* 2002) for all geodetic points of the REGID, RENID and REGRID network processing with respect to the BEGC fundamental geodetic point at Deception Island. The ITRF2000.00 co-ordinates for the BEJC geodetic point were obtained with respect to the IGS Antarctic reference stations OHI2 and PALM. iii) Orthometric height differences between the points of each network must be obtained. In our case, geometric levelling measurements were made between the stations of the REGID network, the benchmarks of the RENID network and the set of auxiliary gravimetric points of the REGRID network, taking the levelling benchmark LN00 as the reference point. iv) Relative gravimetric values must also be obtained. For Deception Island, relative gravimetric measurements were obtained for the REGID network stations, the benchmarks of the RENID network and the secondary points set. The gravimetric base was GRAV (Fig. 5).

The datasets must be filtered and processed, and the equipment used in this work must be compliant with geodetic specifications, which are briefly described below.

The REGID geodetic network

The REGID geodetic network is formed by 12 stations distributed all around the island (Fig. 2), COLA at Colatinas Point, GEOD in the surroundings of Soto Crater, BEGC near the Spanish Gabriel de Castilla Base, BARG at the Argentinian Deception Station, FUMA at Fumaroles Bay, UCA1 at Obsidian Hill, TELE and BOMB flanking Telephon Bay, CR70 in the area of the craters of 1970, PEND at Pendulum Cove, GLAN in the surroundings of the Black Glacier and BALL at Whalers Bay. The LN00 geodetic benchmark was also included as an elevation reference station for the network (Berrocoso *et al.* 2006, 2008). The design and establishment of the network were planned according to Seeber (2003) and the special characteristics of Deception Island because the topographical conditions restrict the building of stations to areas near the coast.

The REGID geodetic network has been surveyed since 1988 in successive Antarctic campaigns. It has been used for the study of models of horizontal deformation due to the volcanic and tectonic activity on the island (Berrocoso *et al.* 2008, Prates *et al.* 2013). The data used to obtain the ellipsoidal heights were obtained between November 2002 and February 2003 (Berrocoso *et al.* 2006, 2008).

The GPS data for positioning of benchmarks and stations were taken from Berrocoso *et al.* (2008). The geodetic stations have absolute co-ordinates in X, Y, Z, and latitude (φ), longitude (λ) and ellipsoidal height (h) relative to ITRF2000.00 with millimetre accuracy (Altamimi *et al.* 2002).

Leica GX1230 and TRIMBLE 5700 receivers were employed with an accuracy (RMS) equal to 5 mm + 0.5 ppm in horizontal and 10 mm + 0.5 ppm in vertical for static surveying (phase) in post-processing and standard antenna. In the first campaign (1989–90) there were 28 days of observation which has since increased to an average of 41 days of observation per campaign.

In order to obtain precision in millimetres, the GNSS-GPS observations were made by the static positioning method with specifications for geodetic surveying according to Seeber (2003, p. 358–362). For this type of surveying it is necessary to have at least one reference station with known precise absolute co-ordinates. The IGS stations OHI2, located at the Chilean O'Higgins Station (Antarctic Peninsula), and PALM, located at the American Palmer Station (Anvers Island), were used as references in a first step. From these stations the absolute geocentric co-ordinates were obtained for BEGC station on Deception Island and BEJC on Livingston Island. The second step was the processing and adjustment of the co-ordinates of the remaining stations on Deception Island, made with respect to BEGC and BEJC (Berrocoso *et al.* 2008). Observation sessions of at least 24 hours were programmed, data were registered with a 1 second sampling rate and the elevation mask was set to 10°. For processing and network adjustment, BERNESE version 5.0 GPS Software (Hungentobler *et al.* 2001) was used to obtain a relative position of the network,

https://doi.org/10.1017/S0954102015000681 Published online by Cambridge University Press

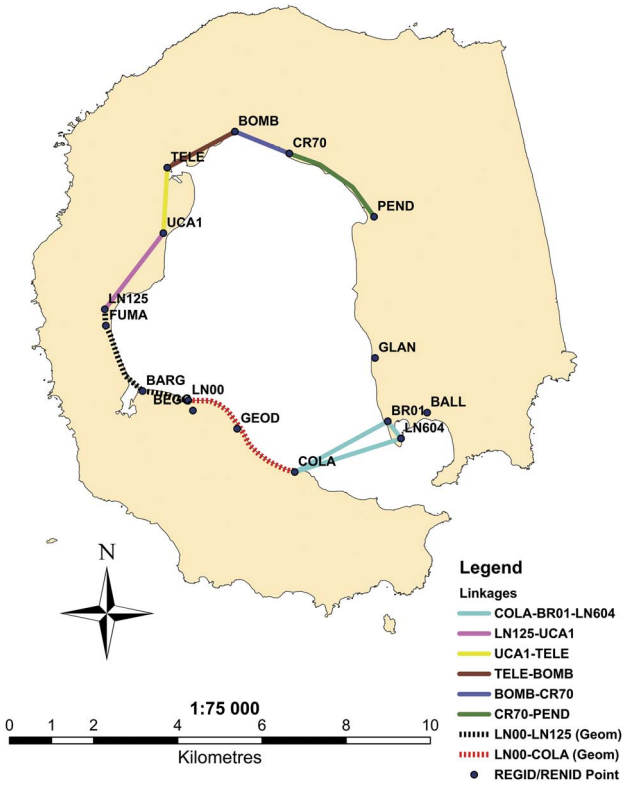

Fig. 7. Linkages between levelling lines of the RENID network.

with respect to the BEGC and BEJC reference stations. In data processing IGS precise orbits and pole files were used for the entire procedure. Baselines were processed using the methodology suggested for GPS data processing in Antarctic regions by Bouin & Vigny (2000). The adjusted co-ordinates of the REGID geodetic network are shown in Table S1 (found at http://dx.doi.org/10.1017/S0954102015000681).

The geodetic benchmarks were constructed with concrete, well-rooted in the permafrost with steel bars and a low height above the ground. A 0.05 m stainless steel screw for the benchmark materialization was fixed in the concrete. Moreover, to ensure the correct and known position of the GNSS-GPS antenna centre with respect to the benchmark at each campaign, a laboratory measured prolongation of nearly 0.13 m was applied to attach the antenna, for more details see the scheme presented for REGID points in Prates *et al.* (2013, fig. 2b).

The RENID levelling network

The RENID levelling network consists of 60 benchmarks and it is divided into six independent levelling lines. The fundamental benchmark is LN00, situated near the Gabriel de Castilla Station. The orthometric height of LN00 was determined by a geometric levelling from the COLA geodetic benchmark, with the orthometric height provided from the works carried out by Vidal *et al.* (2012) and Jigena *et al.* (2014). Every line is connected to one of the geodetic stations of the REGID network except levelling line 4, which is connected to the fundamental benchmark LN00. Figure 4 shows the levelling lines and the REGID network which are linked.

Levelling surveys of the RENID networks were carried out during the 2001–02 and 2002–03 campaigns. The geometric levelling was undertaken using a Leica optical level model NA2 with an accuracy of ± 0.7 mm km^{-1} double run levelling. A Leica TPS 403 Total Station was used in the trigonometric levelling and geodetic linkages. The Leica TPS 403 Total Station has a 1" resolution in angular reading with a standard deviation of 3" for horizontal and vertical angles, and 2 mm + 2 ppm precision in distances over the 3500 m maximum distance with a Leica GPR1 prism. Corrections due to sphericity and refraction effects were applied to the data. The fundamental geodetic benchmarks have the height above mean sea level reference, relative to the COLA geodetic vertex and LN00 benchmark on Deception Island, and relative to the BEJC geodetic vertex on Livingston Island, all of which are referred according to the results obtained by Jigena *et al.* (2014). On Deception Island, the orthometric height obtained for COLA was translated to LN00 by geometric levelling, obtaining a closing error of 13.0 mm for 7.209 km over the total levelling distance, within the second order geodetic levelling. The LN00 point has been defined as the fundamental geodetic benchmark of the REGID levelling network in Berrocoso *et al.* (2008). Table S2 shows the obtained levelling data as well as their associated errors (found at http://dx.doi.org/10.1017/S0954102015000681).

The levelling lines are independent and the elevation of the benchmarks, belonging to each line, were obtained by geometric levelling. However, the linkages between the levelling lines were performed by a trigonometric levelling method, taking measurements with a Leica Total Station model TPS-403, except for the linkage between COLA and LN00 which was performed by geometric levelling. The locations of the linkages are shown in Fig. 8 and the results obtained for the different linkages are shown in Table S3 (found at http://dx.doi.org/10.1017/S0954102015000681).

The 48 benchmarks of the RENID network were placed over concrete blocks on volcanic rock. The points over the concrete blocks were made according to a scheme presented for REGID points, with a block size of 0.30 × 0.30 m. Benchmarks placed on volcanic rock were constructed with a block of epoxy resin with a 0.12 m base and a height of 0.14 m. The resin block was fixed to the rock by a variable height stainless steel screw and the physical materialization of the geodetic reference point on the benchmark is the top of the screw. Figure S1 (found at http://dx.doi.org/10.1017/

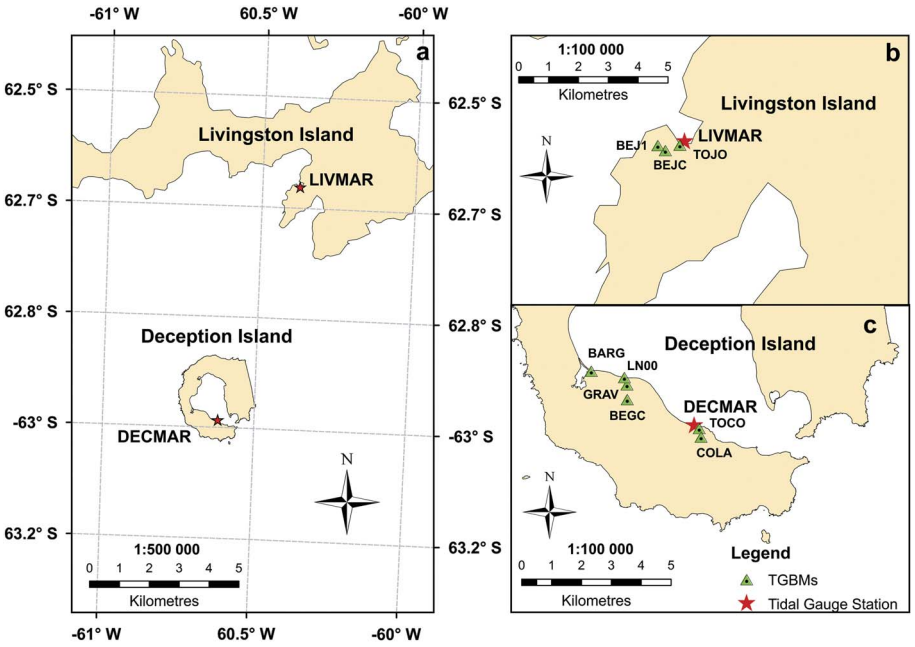

Fig. 8a. Location of tidal gauge stations on Livingston and Deception islands. Detailed maps showing the tidal gauge stations and their related tidal gauge benchmarks on **b.** Livingston Island and **c.** Deception Island.

S0954102015000681) shows the levelling marks of the RENID network fixed on volcanic rocks.

The REGRID gravimetric network

The REGRID gravimetric network was established in 2002–03 using 12 geodetic stations of the REGID network, 50 levelling benchmarks of the RENID network and 46 auxiliary gravimetric points with a total of 108 gravimetric points on Deception Island (Fig. 5). The fundamental gravimetric point on Deception Island was set up to be GRAV (Berrocoso *et al.* 2008). Another gravimetric point at Deception Island was TOCO, which is the tidal gauge benchmark (TGBM) for control of the DECMAR tidal station.

The gravimetric points on Livingston Island (BEJC, BEJ1 and TOJO) were also included in the network. BEJC is the fundamental gravimetric point on Livingston Island, BEJ1 is the new geodetic vertex and TOJO is the tide gauge auxiliary benchmarks (TGABs) for the LIVMAR tidal station. The three points on Livingston Island are situated in the surroundings of the Spanish Juan Carlos I Base (Fig. 8).

The gravimetric connection between the South American continent and the South Shetland Islands was conducted in 2002–03. The gravimetric base APPA, located at Punta Arenas (Chile) and pertaining to the Chilean Gravimetric Network, was used as the fundamental gravimetric base. The gravity value taken at APPA was 981320.81 mGal. The connection was made from APPA to BEJC (Livingston Island) and GRAV (Deception Island) geodetic stations (Berrocoso *et al.* 2008). The closing of the gravimetric survey was made on the return to South America. The gravity values are shown in Table I.

The fundamental gravimetric point on Deception Island was set up to be GRAV. We included one gravimetric reference point (BEJC) in the network on Livingston Island. Gravimetric measurements were obtained with a Lacoste & Romberg D-203 relative gravimeter, which has a reading precision of ± 0.01 mGal and a static drift of < 1 mGal per month (Berrocoso *et al.* 2008). Tides, height and drift corrections were applied to the whole set of gravimetric data. The correction for tides was calculated for an average latitude of Deception Island ($\gamma = 62°57'30''$), constructing a daily correction curve which was applied with its sign to each reading of the gravimeter. The derived correction was controlled by means of the readings made in the base or reference station at the beginning and end of each circuit, assuming that it is linear given that the time between each circuit was generally less than six hours. The correction was distributed proportionally on each circuit, according to the hour of measurement at the station throughout the circuit, obtained with the sign to apply. The correction for tide and drift was made according to Martín-Furones (2000). The correction for altitude, due to the variation in

Table I. Gravity values obtained for the link between the South American continent and the gravimetric bases of Livingston and Deception islands.

Gravimetric base (linkage)	Gravity value (mGal)	Standard deviation (mGal)	Number of linkages
APPA	981320.8100	0.0150	1
BEJC	982212.8190	0.1374	1
GRAV	982202.5445	0.1866	1

https://doi.org/10.1017/S0954102015000681 Published online by Cambridge University Press

Table II. REGRID network. Gravimetric measurements and estimated errors (sigma).

#	Station	Gravity (mGal)	σG (mGal)	#	Station	Gravity (mGal)	σG (mGal)
1	LN00	982206.408	0.051	32	LN117	982205.665	0.060
2	BEGC	982196.927	0.021	33	LN118	982204.907	0.077
3	BALL	982204.414	0.027	34	LN119	982204.957	0.092
4	FUMA	982204.912	0.026	35	LN120	982204.608	0.094
5	PEND	982202.237	0.022	36	LN121	982204.254	0.092
6	COLA	982205.580	0.035	37	LN122	982204.026	0.086
7	GLAN	982201.404	0.040	38	LN123	982203.253	0.075
8	GEOD	982203.666	0.028	39	LN124	982204.803	0.058
9	UCA1	982201.949	0.029	40	LN125	982205.356	0.087
10	CR70	982201.672	0.032	41	LN201	982200.860	0.078
11	TELE	982204.877	0.034	42	LN202	982202.898	0.078
12	BOMB	982204.710	0.038	43	LN203	982202.238	0.087
13	GRAV	982202.545	0.006	44	LN301	982200.833	0.056
14	BARG	982206.942	0.018	45	LN302	982199.515	0.061
15	TOCO	982205.580	0.006	46	LN303	982202.097	0.051
16	LN101	982205.937	0.059	47	LN401	982206.461	0.053
17	LN102	982204.751	0.052	48	LN402	982205.851	0.064
18	LN103	982206.520	0.058	49	LN403	982204.553	0.065
19	LN104	982207.415	0.077	50	LN404	982202.775	0.054
20	LN105	982206.059	0.089	51	LN501	982203.602	0.071
21	LN106	982207.936	0.096	52	LN502	982200.069	0.075
22	LN107	982205.767	0.100	53	LN503	982198.328	0.057
23	LN108	982206.612	0.102	54	BR-01	982200.614	0.053
24	LN109	982205.950	0.100	55	LN601	982205.191	0.049
25	LN110	982203.095	0.096	56	LN602	982204.490	0.051
26	LN111	982202.109	0.089	57	LN603	982203.097	0.052
27	LN112	982204.271	0.077	58	LN604	982205.008	0.050
28	LN113	982206.870	0.059	59	LN605	982202.019	0.066
29	LN114	982206.167	0.053	60	LN606	982202.965	0.068
30	LN115	982206.008	0.061	61	LN607	982200.233	0.050
31	LN116	982205.614	0.054	62	LN608	982201.389	0.061

the height above mean sea level between the reference point and the measurement station, the Free-Air correction and the Bouguer correction were applied according to that specified by Heiskanen & Moritz (1967). Gravimetric values and the estimated errors are displayed in Table II.

The orthometric heights (H) were calculated from the ellipsoid height (h), obtained from the GPS measurements, absolute gravity measurements (g) and the geometric levelling differences (Δn), according to Heiskanen & Moritz (1967) and Berrocoso *et al.* (1996, 2008).

Sea level measurements were linked to fixed onshore benchmarks by comparing simultaneous readings of the gauges against a previously levelled shore-based tidal staff. Using precise geodetic levelling, the heights of TGBMs were calculated relative to the heights of nearby geodetic stations, COLA and LN00 on Deception Island and BEJC geodetic vertex on Livingston Island, calculating the new values of orthometric height according to the results obtained by Jigena *et al.* (2014). The TGBMs TOCO (Deception Island) and TOJO (Livingston Island) were used as benchmarks from which the orthometric levels of nearby geodetic stations, COLA and LN00 at Deception Island and BEJC at Livingston Island, were obtained. The final values of gravimetric measurements on Deception Island are shown in Table II.

Complementary observations

Complementary measurements were carried out on the Deception Island networks in order to use all the stations and benchmarks.

In addition to the GPS observations, levelling and gravimetric measurements, the stations of the REGID network were linked to the RENID network by geometric or trigonometric levelling (see Fig. 7). These stations are thus provided with levelling measurements and the new values were adjusted with respect to the fundamental benchmark LN00 (see Table S2). Similarly, every levelling benchmark is provided with geodetic co-ordinates obtained by static positioning with BEGC as the reference station. Further, every benchmark in the REGRID network is provided with geodetic co-ordinates obtained by GPS, an absolute gravity value and levelling measurements.

The adverse geographical conditions of Deception Island, with glaciers near the shore and the inaccessible outer coast, forced the REGID, RENID and REGRID

https://doi.org/10.1017/S0954102015000681 Published online by Cambridge University Press

networks to be developed around the inner bay, not further than 1 km from the coast line (as shown in Fig. 7). In order to spread the observations to the outer area and to make the measurement set more dense, 46 secondary points were also established (Fig. 5) and GPS observations, levelling and gravimetric measurements were obtained for these marks, as shown in Table S4 (found at http://dx.doi.org/10.1017/S0954102015000681).

Every point was positioned in fast-static mode, using a TRIMBLE 5700 dual frequency receiver, while levelling tasks were carried out using a Leica TPS-403 Total Station, as seen for the REGID, RENID and REGRID networks.

Measurements on Livingston Island

On Livingston Island, a new and more accurate orthometric height is provided for the geodetic vertex BEJC, pertaining to the Red Geodésica Antártica Española (RGAE) network and the REGID network. Other geodetic benchmarks on the island are BEJ1 and TOJO. These two points have served to determine the levelling height relative to mean sea level, with respect to BEJC, and to later determine the geoid undulation (*N*) in the area surrounding the Juan Carlos I Base. Installed in 1987–88, the BEJC geodetic station is the fundamental geodetic point on Livingston Island and pertaining to the RGAE network. A new BEJ1 geodetic vertex was installed to replace the previous one which was affected by the construction of the Juan Carlos I Base. The TOJO geodetic benchmark, which is the TGAB point of control of the LIVMAR tidal station at Johnsons Dock, was also used. For more details of the locations of the geodetic marks see Figs 1 & 8.

In order to establish these three geodetic points, the following specifications were considered: i) The ITRF 2000.00 co-ordinates of the BEJC geodetic point were obtained with respect to the OHI2 and PALM IGS stations. The GPS solutions to be given in ITRF2000.00 co-ordinates for all stations. ii) The co-ordinates for all geodetic points on Livingston Island were processed with respect to the BEJC geodetic vertex and the BEGC fundamental geodetic point at Deception Island. iii) Geometric levelling for BEJ1 and TOJO were taken with respect to the levelling benchmark BEJC as reference

Table III. Mean geoid undulation (*N*) and corresponding errors (standard deviation) for GeoiDEC14.

#	Station	N_{2014} (m)	σN_{2014} (m)	#	Station	N_{2014} (m)	σN_{2014} (m)	#	Station	N_{2014} (m)	σN_{2014} (m)
1	LN00	18.93	0.06	35	LN122	18.59	0.09	69	EG11	18.93	0.16
2	BEGC	18.74	0.06	36	LN123	18.09	0.08	70	EG13	18.91	0.16
3	BALL	19.16	0.09	37	LN124	18.65	0.08	71	EG14	18.93	0.16
4	FUMA	19.49	0.07	38	LN125	18.55	0.07	72	G02	18.47	0.16
5	PEND	19.08	0.10	39	LN201	18.93	0.07	73	G03	18.49	0.16
6	COLA	18.92	0.08	40	LN202	18.90	0.07	74	G04	18.56	0.16
7	GLAN	19.08	0.10	41	LN203	18.88	0.08	75	G07	18.83	0.16
8	GEOD	18.90	0.08	42	LN301	18.98	0.11	76	G10	18.87	0.16
9	UCA1	18.98	0.10	43	LN302	18.92	0.11	77	G14	19.31	0.16
10	CR70	18.96	0.12	44	LN303	19.14	0.10	78	G15	19.25	0.16
11	TELE	18.99	0.14	45	LN401	18.39	0.07	79	G16	19.22	0.16
12	BOMB	18.98	0.09	46	LN402	18.61	0.08	80	G17	18.83	0.16
13	GRAV	18.90	0.07	47	LN403	19.03	0.10	81	G18	18.90	0.16
14	LN101	18.93	0.06	48	LN404	18.72	0.09	82	G20	18.84	0.16
15	LN102	18.89	0.07	49	LN501	18.74	0.14	83	G21	18.78	0.16
16	LN103	18.92	0.07	50	LN502	18.53	0.13	84	G22	18.84	0.16
17	LN104	18.96	0.08	51	LN503	19.04	0.13	85	G26	18.94	0.16
18	LN105	18.90	0.08	52	BR-01	18.18	0.10	86	G27	18.88	0.16
19	LN106	18.94	0.07	53	LN601	18.68	0.13	87	G28	19.01	0.16
20	LN107	18.92	0.07	54	LN602	18.51	0.12	88	G31	18.82	0.16
21	LN108	18.91	0.06	55	LN603	18.71	0.11	89	G32	18.86	0.16
22	LN109	18.91	0.07	56	LN604	18.14	0.12	90	G33	18.93	0.16
23	LN110	18.88	0.07	57	LN605	18.27	0.12	91	G34	18.91	0.16
24	LN111	18.89	0.07	58	LN606	19.01	0.12	92	G35	18.95	0.16
25	LN112	18.94	0.07	59	LN607	18.35	0.15	93	G42	18.99	0.16
26	LN113	18.94	0.07	60	LN608	18.70	0.14	94	G43	18.92	0.16
27	LN114	18.94	0.07	61	EG01	19.96	0.16	95	G44	18.88	0.16
28	LN115	18.61	0.08	62	EG02	18.80	0.16	96	G45	18.90	0.16
29	LN116	18.59	0.09	63	EG03	19.09	0.16	97	G48	18.99	0.16
30	LN117	18.96	0.08	64	EG05	19.25	0.16	98	G49	19.04	0.16
31	LN118	18.36	0.08	65	EG06	18.87	0.16	99	G53	18.91	0.16
32	LN119	18.05	0.09	66	EG07	18.81	0.16	100	G55	18.86	0.16
33	LN120	18.17	0.09	67	EG09	18.94	0.16	101	G57	18.87	0.16
34	LN121	18.69	0.09	68	EG10	18.89	0.16	102	TOCO	19.01	0.07

Table IV. Mean geoid undulation (N) and corresponding errors (standard deviation) for Livingston Island.

#	Station	Latitude S	Longitude W	N_{2014} (m)	σN_{2014} (m)
201	BEJC	62°39'46.7792	60°23'19.9940	18.808	0.085
202	BEJ1	62°39'46.4427	60°23'16.6494	18.905	0.087
203	TOJO	62°39'35.6708	60°22'30.1424	18.917	0.101

point. iv) Relative gravimetric measurements at the stations were set relative to the BEJC gravimetric base.

Tide gauge benchmark control points

The TGBMs for control of tide gauge stations were also used for the geoid calculation. These geodetic benchmarks are COLA and LN00 on Deception Island and BEJC on Livingston Island. The levelling heights relative to mean sea level for COLA, LN00 and BEJC were provided using the TGABs TOCO, located at Colatinas Point (Deception Island), and TOJO, located at Johnsons Dock (Livingston Island). For a more detailed explanation see Vidal *et al.* (2012, fig. 2), Jigena *et al.* (2014) and Figs 1 & 8.

The mean sea level results obtained for the geodetic reference stations were 12.42 m a.m.s.l. for BEJC and 29.05 m a.m.s.l. for COLA, and the associated errors were ± 0.08 m and ± 0.05 m, respectively (Jigena *et al.* 2014). The fundamental benchmark on Deception Island was LN00, the orthometric height value of which was 6.20 m a.m.s.l. with an error ± 0.088 m. These values were taken as fundamentals for the new height calculation and adjustment of the REGID, RENID and REGRID networks, improving their precision. These new values were also used in the calculations and determination of the experimental geoid for Deception Island, GeoiDEC14.

Results

A precise geoid, GeoiDEC14, was obtained for Deception Island, as well as three geodetic benchmarks providing values of geoid undulation (N) for the area around the Juan Carlos I Base and Johnsons Dock.

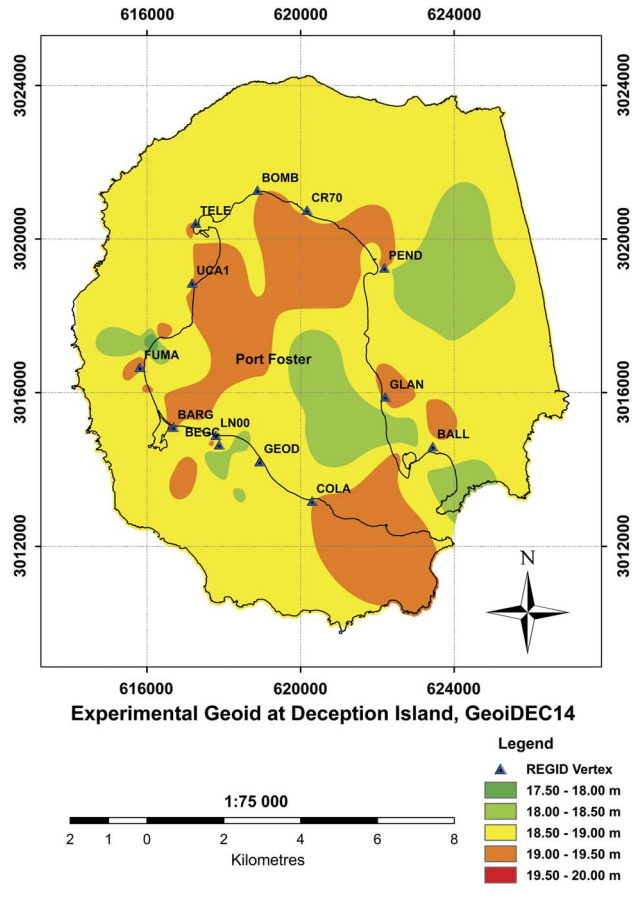

Fig. 9. Experimental geoid, GeoiDEC14, at Deception Island.

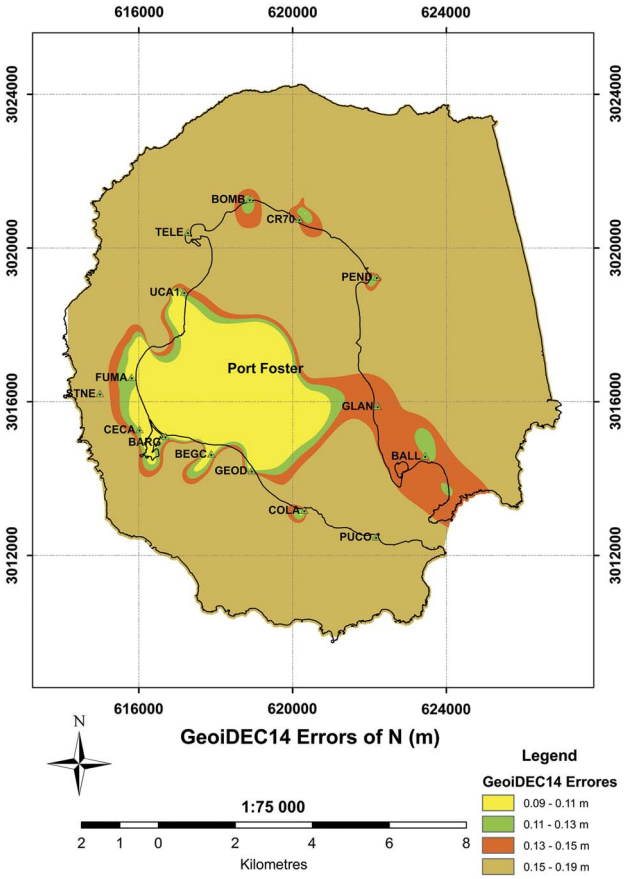

Fig. 10. Estimated GeoiDEC14 errors of N. The contour map was obtained using ArcGIS 9.3 software from Esri (2008).

https://doi.org/10.1017/S0954102015000681 Published online by Cambridge University Press

Table V. Estimated GeoiDEC14 errors grouped by area of interest.

Area	Error (m)
Colatinas Point, Gabriel de Castilla Base, Fumarole Bay, Obsidianas Field, Pendulum Cove	0.09–0.11
Bombs Field, CR70 Field, Black Glacier	0.11–0.15
Telephon Bay, Collins Point, Lobera Beach	0.15–0.19

The mean geoid undulations and the estimated errors for GeoiDEC14 and Livingston Island are shown in Tables III & IV, respectively.

Figure 9 shows the geoid undulation (N) of the experimental geoid GeoiDEC14 at Deception Island.

Figure 10 shows a contour map produced by interpolating these data, as well as the errors, for the whole island using the Spline Tension method, which controls the stiffness of the surface according to the character of the modelled phenomenon creating a less smooth surface with values more closely constrained by the sample data range.

The estimation of errors was made by applying Eqs (3, 4 & 5) and the law of errors propagation. Thus the levelling errors have been added to the error obtained for the determination of mean sea level, which is 0.051 m for the COLA benchmark. The error map (Fig. 10) only shows the error propagation without taking into account errors due to the interpolation technique. The errors in GeoiDEC14, estimated according to Eq. (3), do not exceed 0.19 m and can be grouped into three areas (Table V). Note that the greatest errors were obtained at CR70, Pendulum Cove and Collins Point, while a trend change was observed at Whalers Bay that can be attributed to a better fit network due to mixed linkage (geometric and trigonometric levelling) between the COLA geodetic vertex and the LN604 and BR01 geodetic benchmarks placed near BALL (Whalers Bay; see Fig. 7).

Furthermore, three points fitted with geoid undulation (N), elevation and GNSS absolute co-ordinates were obtained for the areas surrounding the Juan Carlos I Base and Johnsons Dock. As the points are very close the solution is not relevant for cartographic representation and not sufficient for the determination of a local geoid in this area. The error estimated in the elevation determination regarding mean sea level for BEJC was 0.088 m. This error was extrapolated to all points, adding it to the errors obtained in the geometric levelling. Table IV shows the results of these observations on Livingston Island and the locations of the stations are shown in Fig. 8b.

Discussion

The importance of this work lies in it being the first model of a precise local geoid obtained for the volcanically active Deception Island. The geoid will enable technical and scientific work to be undertaken and to produce results with a high level of precision at the island. The geoid can be used for the calibration of global geopotential models, as well as for the direct determination of orthometric heights, combining the model with GPS observations. Furthermore, the data will be helpful in volcanic

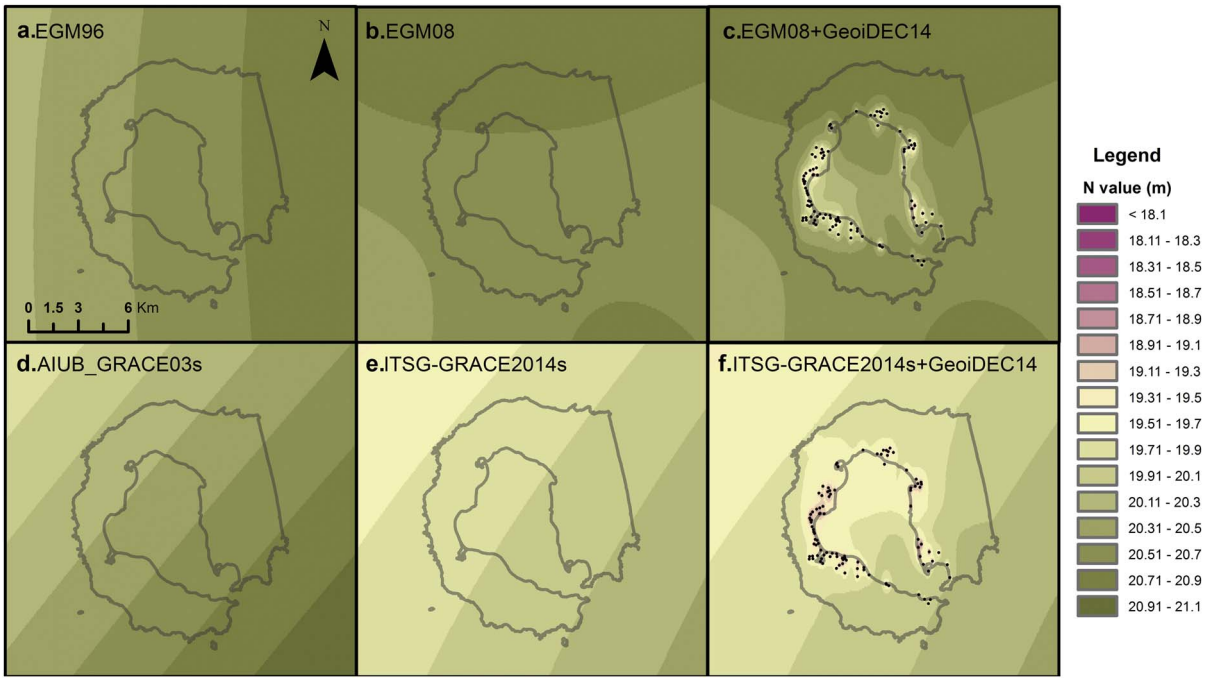

Fig. 11. Undulation values (N) according to **a.** EGM96, **b.** EGM08, **d.** AIUB_GRACE03s and **e.** ITSG-Grace2014s. **c.** and **f.** show the insertion of GeoiDEC14 within EGM08 and ITSG-Grace2014s.

https://doi.org/10.1017/S0954102015000681 Published online by Cambridge University Press

Table VI. Statistical summary of *N*, in metres, for global geopotential models and DEC2007 versus GeoiDEC14. ES_Max and ES_Average is the result of effect size (ES) analysis.

	A. Statistical summary						B. Difference relative to GeoiDEC14				
	GeoiDEC14	DEC2007	EGM96	AIUG-Grace03s	EGM2008	ITSG-Grace2014s	EGM96	AIUG-Grace03s	EGM08	ITSG-Grace2014s	DEC2007
Maximum	19.49	20.37	20.69	20.70	20.73	20.08	-0.96	-0.81	-1.12	-0.32	0.26
Minimum	18.05	18.77	20.44	20.23	20.57	19.78	-2.51	-2.52	-2.57	-1.90	-1.85
Mean	18.82	19.64	20.53	20.40	20.64	19.88	-1.71	-1.58	-1.81	-1.06	-0.82
Standard deviation	0.26	0.28	0.08	0.13	0.05	0.08	0.28	0.30	0.26	0.28	0.23
ES_Max	0.00	4.56	4.58	4.69	2.25	3.35					
ES_Average	0.00	6.45	5.97	6.86	4.00	3.10					

deformation models for designing lava flow models to determine hazard maps and identifying or defining risk areas, in oceanography for the control of sea levels, and in direct surveying with GPS and geophysical applications.

For the determination of the geoid of Deception Island, gravity observations were made on the vertices of the REGRID network, which includes all the points of the REGID geodesic network and the RENID levelling network, all with ITRF2000.00 co-ordinates and orthometric heights. To obtain the precise local geoid model, GeoiDEC14, a GPS/levelling/gravity methodology was used, with a total of 108 points available on Deception Island distributed homogenously in the interior part of the island around Port Foster. These points have an average value in geoid undulation (*N*) of 18.83 m, with a maximum of 19.49 m and minimum of 18.05 m.

Three further points were measured on Livingston Island with an average of 18.87 m, similar to that of Deception Island, giving validity to the results.

The geoid heights were obtained from several global geopotential models in order to present and analyse the differences with respect to the experimental geoid GeoiDEC14. The EGM96 (Lemoine *et al.* 1998), EGM2008 (Pavlis *et al.* 2012), AUIB-GRACE03s (Pail *et al.* 2010, Fecher *et al.* 2015), ITSG-Grace2014s (Mayer-Guerr *et al.* 2014) and a local experimental geoid of Deception Island obtained in 2007, DEC2007 (Berrocoso *et al.* 2006) were selected. Figure 11 shows the comparisons according to interpolated data obtained from a grid of 0.001° using the tools of the Calculation Service of the International Centre for Global Earth Models (ICGEM). GeoiDEC14 has been introduced in Fig. 11c & f to show its influence in the EGM08 and ITSG-Grace2014s geoids. GeoiDEC14 reduces the undulation value of the geoid in some areas to values of 18 m (dark pink colour in Fig. 11), a value not reached in any of the studied global geoids.

Specifically, this comparison shows a maximum difference of the minimum *N* value, determined at the observed points, of *c*. 2.50 m with respect to the previous global models EGM96, EGM08 and AUIB-Grace03s (Fig. 11a, b & d) and 1.90 m with respect to the most modern DEC2007 and ITSG-Grace2014s (Fig. 11e), see Table VI. The maximum values also differ between both groups, with the maximum value in our geoid between 0.81 m and 1.12 m lower with respect to EGM96, AUIB-Grace03s and EGM08, and increasing to ± 0.32 m with respect to ITSG-Grace2014s and DEC2007.

GeoiDEC14 generally presents lower *N* values compared to the other geoids, and in all cases the maximum value of GeoiDEC14 is lower than the mean for the other geoids (Table VI). Furthermore, the difference relative to GeoiDEC14 for the global models ranged from -1.81 m to -0.82 m, showing a better fit for GeoiDEC14 with the latter two models. The standard deviations remain very similar in all of the global models.

The relatively small difference (0.82 m in Table VI) with respect to the DEC2007 experimental model may be due to the use of the same methodology in this model but with fewer data; DEC2007 also lacked a vertical reference level (mean sea level). The new data presented here were obtained with greater precision. With respect to the closeness of GeoiDEC14 to ITSG-Grace2014s, this could be due to the higher resolution of this model (200 order). The comparison shows a significant level of improvement in the accuracy of our model with respect to the global models and the previous experimental model in the local area.

When the global models are compared to the EIGEN6C4 geoid, the latest geoid offered by the German Research Centre for Geoscience (GFZ), the difference does not exceed 0.15 m for EGM08 (160 order), 0.30 m in the worst case for ITSG-Grace2014s (200 order) and 0.05 m for AIUG-Grace03s (160 order). The reference data, which GFZ offers with respect to 12 224 GPS-levelling points (from Canada, the USA, Europe, Japan and Australia), present an RMS of 0.43 m, 0.66 m, 0.24 m and 1.05 m for EGM96, AIUG-Grace03s, EGM2008 and ITSG-Grace2014s, respectively. These RMSs are lower than the differences shown in Table VI for the different models, so there is another reason for these values. The best adjustment with ITSG-Grace2014s is due to the high resolution of this geopotential model, which is the last one made available to the scientific community and has GRACE data of more than 10 years for its

https://doi.org/10.1017/S0954102015000681 Published online by Cambridge University Press

determination. The model also includes data on the atmosphere and the oceanic mass. Therefore, a higher resolution global model could reduce the difference.

An effect size (ES) analysis (Ledesma *et al.* 2008) was carried out on the comparisons made for the different models. The estimation of ES is considered a necessary complementary test of a hypothesis between a model whose validity needs to be proved (M_0), in this case our GeoiDEC14 model, and the reference models (M_1). The maximum for each of the models, which would be the worst case scenario, and the mean, which would be the most representative value in each model, were taken as study parameters. The models where the ES is smallest would be those that more closely approach our model pattern. For our case, the results indicate that the smallest values correspond to ITSG-Grace2014 and DEC2007, again marking this separation between models and confirming that these are the models with the greater precision and resolution among those compared. They validate the hypothesis that the local geoid model GeoiDEC14 is the most precise geoid model obtained to date for Deception Island.

The comparison of the distribution of the *N* values in GeoiDEC14, shows that some of the anomalies coincide with hot spots on the island. The minimum values shown in Fumarole Bay and Whalers Bay, which are areas with active fumaroles, or the maximum values found in the remains of lava at Colatinas, Black Glacier or Murature Point are some examples (Fig. 9). These anomalies may be due to the properties of the crust and the density of the ground in the area (Crescentini & Amoruso 2007).

Finally, a new and more accurate orthometric height and geoid undulation (*N*) are provided for geodetic stations BEJC and BEJ1, and the tide gauge control station TOJO on Livingston Island. The values are similar to the those obtained for Deception Island. Livingston Island has no volcanic activity, offering very similar *N* values between the three points, and therefore no anomaly. Although these three values do not allow a geoid to be determined in the area, they do serve as a comparison for values obtained on Deception Island. The results suggest that the crustal structure and mass distribution are broadly comparable on both islands.

Conclusions

A precise geoid model for Deception Island has been derived by means of a direct GPS-levelling technique from a combination of GPS, levelling and gravimetric data in order to obtain geoid undulation data with a greater precision than that obtained previously, including existing global models. The new local model, GeoiDEC14, through greater precision, allows the orthometric heights to be determined directly. Thus, it can be used in geophysical, topographical and oceanographic applications throughout our area of study, mainly in the interior area of the island around Port Foster.

The results of the studies on the mean sea level obtained at the tide gauge stations of LIVMAR (Livingston Island) and DECMAR (Deception Island) have been introduced in the new calculation and adjustment of the REGID, RENID and REGRID, and in the calculation of the new precision geoid of Deception Island, GeoiDEC14. These were the first vertical reference levels obtained on the basis of real mean sea level data taken *in situ*. The introduction of these new data has provided a highly precise geoid model (maximum error of 0.2 m) and has noticeably improved the precision previously obtained by similar models in the area (DEC2007), as well as on that of global models.

Comparing our experimental model with global geoid models, the geopotential model ITSG-Grace2014s presents a best fit with respect to our model. Furthermore, the results are improved compared to the experimental model DEC2007. In terms of comparing the level of adjustment of different geoid models with that obtained in this work, we conclude that the ITSG-Grace2014s geopotential model shows good agreement with the experimental geoid GeoiDEC14, with a difference in average values of -1.06 m, whereas with the other global models the difference is > -1.58 m. The agreement with ITSG-Grace2014s is probably due to the high resolution of this geopotential model.

Data were calculated for three geodesic stations on Livingston Island providing the geoid undulation, in addition to the corresponding geodetic data. These three values do not allow the determination of a geoid in the area, nevertheless they serve as a comparison to the Deception Island data. It can be concluded that the mean geoid undulation values are similar to those obtained for Deception Island, which validate our local geoid model, GeoiDEC14.

It must be acknowledged that this experimental geoid, GeoiDEC14, could be improved by i) adding data from the outer area of the island, since the geoid height for the outer coast was obtained by extrapolating the values taken near the inner bay, and ii) the addition of marine gravimetric measurements. Furthermore, it is advisable to conduct a new levelling survey in order to correct the altimetric reference framework errors defined in 2003, to redefine a new framework with an improved accuracy. The possibility of adding radar altimeter data for instantaneous sea level measures should also be considered.

Acknowledgements

This work was made possible by the support of the following projects, funded by the Spanish Ministry of Science and Technology through the National Programme of Antarctic Research and Natural Resources REN2000-0551-C03-01/ANT, REN2002-1383/ANT, CGL2004-21547-E/ANT, CGL2007-28768-E/ANT, CTM2008-03113-E/ANT and CTM2009-07251/ANT, as

well as the Research Group RNM314 Geodesia y Geofísica Cádiz, pertaining to the Junta de Andalucía, Spain. The authors thank the crew of the Oceanographic Research Vessel *BIO Las Palmas* and the members of the Spanish Antarctic stations Gabriel de Castilla and Juan Carlos I for their collaboration during the surveying campaigns. We also thank Dr Jorge Gárate for comments and suggestions in the production of this paper. The authors thank the editors, Professor Smellie, Professor Zanutta and an anonymous reviewer for their comments which greatly improved the manuscript.

Author contributions

Research design: MBD, BJA, CTL, AFR and JVP. Data collection (participating in the Spanish Antarctic campaigns 1989–2013): MBD, BJA, CTL, JVP, AFR and IBG. Data processing and manuscript preparation: BJA, CTL, MBD, IBG, AFR and JVP. Manuscript final editing: BJA, CTL, MBD, AFR, IBG and JVP.

Supplemental material

Supplemental tables and a figure will be found at http://dx.doi.org/10.1017/S0954102015000681.

References

Altamimi, Z., Sillard, P. & Boucher, C. 2002. ITRF2000: a new release of the International Terrestrial Reference Frame for earth science applications. *Journal of Geophysical Research - Solid Earth*, **107**, 10.1029/2001JB000561.

Berrocoso, M., Torrecillas, C., Jigena, B. & Fernández-Ros, A. 2012. Determination of geomorphological and volumetric variations in the 1970 land volcanic craters area (Deception Island, Antarctica) from 1968 using historical and current maps, remote sensing and GNSS. *Antarctic Science*, **24**, 367–376.

Berrocoso, M., Gárate, J., Martín-Dávila, J., Fernández-Ros, A., Moreu, G. & Jigena, B. 1996. Improving the local geoid with GPS. *Reports of the Finnish Geodetic Institute*, **96**, 91–96.

Berrocoso, M., Fernández-Ros, A., Torrecillas, C., Enríquez De Salamanca, J.M., Ramírez, M.E., Pérez-Peña, A., González, M.J., Páez, R., Jiménez-Teja, Y., García-García, A., Tárraga, M. & García-García, F. 2006. Geodetic research on Deception Island, Antarctica. *In* Fütterer, D.K., Damaske, D., Kleinschmidt, G., Miller, H. & Tessensohn, F., *eds. Antarctica: contributions to global earth sciences*. Berlin: Springer, 391–396.

Berrocoso, M., Fernández-Ros, A., Ramírez, M.E., Enríquez De Salamanca, J.M., Torrecillas, C., Pérez-Peña, A., Páez, R., García-García, A., Jiménez-Teja, Y., García-García, F., Soto, R., Gárate, J., Martín-Dávila, J., Sanchez-Alzola, A., De Gil, A., Fernández-Prada, J.A. & Jigena, B. 2008. Geodetic research on Deception Island and its environment (South Shetland Islands, Bransfield Sea and Antarctic Peninsula) during Spanish Antarctic campaigns (1987–2007). *In* Capra, A. & Dietrich, R., *eds. Geodetic and geophysical observations in Antarctica*. Berlin: Springer, 97–124.

Bouin, M.N. & Vigny, C. 2000. New constrains on Antarctic plate motion and deformation from GPS data. *Journal Geophysical Research - Solid Earth*, **105**, 28 279–28 293.

Carbó, A., Muñoz-Martín, A., Dávila, J., Catalán, M. & García, A. 2001. Análisis de nuevos datos gravimétricos marinos en el entorno de la Isla Decepción (Islas Shetland del Sur, Antártida). *Revista de la Sociedad Geológica de España*, **14**, 189–197.

CGE (Centro Geográfico Ejército Español) 1992. *Topographic map of Deception Island*. 1:25 000. Madrid: Centro Geográfico Ejército Español.

Crescentini, L. & Amoruso, A. 2007. Effects of crustal layering on the inversion of deformation and gravity data in volcanic areas: an application to the Campi Flegrei caldera, Italy. *Geophysical Research Letters*, **34**, 10.1029/2007GL029919.

Esri 2008. *ArcGIS desktop 9.3 help*. Redlands, CA: Esri.

Fecher, T., Pail, R. & Gruber, T. 2015. Global gravity field modeling based on GOCE and complementary gravity data. *International Journal of Applied Earth Observation and Geoinformation*, **35**, 120–127.

Gracia, E., Canals, M., Farranz, M.L., Sorribas, J. & Pallas, R. 1997. Central and eastern Bransfield basins (Antarctica) from high-resolution swath-bathymetry data. *Antarctic Science*, **9**, 168–180.

Heiskanen, W.A. & Moritz, H. 1967. *Physical geodesy*. New York, NY: W.H. Freeman, 364 pp.

Hungentobler, U., Schaer, S. & Fridez, P., *eds*. 2001. *Bernese GPS Software Version 4.2*. Berne: Astronomical Institute, University of Berne, 32 pp.

Jigena, B., Vidal, J. & Berrocoso, M. 2014. Determination of the mean sea level at Deception and Livingston islands, Antarctica. *Antarctic Science*, **27**, 101–102.

Ledesma, R., Macbeth, G. & Cortada, N. 2008. Tamaño del efecto: revisión teórica y aplicaciones con el sistema estadístico ViSta. *Revista Latinoamericana de Psicología*, **40**, 425–439.

Leick, A. 2004. *GPS satellite surveying*, 3rd ed. Hoboken, NJ: John Wiley, 464 pp.

Lemoine, F.G., Kenyon, S.C., Factor, J.K., Trimmer, R.G., Pavlis, N.K., Chinn, D.S., Cox, C.M., Klosko, S.M., Luthcke, S.B., Torrence, M.H., Wang, Y.M., Williamson, R.G., Pavlis, E.C., Rapp, R.H. & Olson, T.R. 1998. *The development of the joint NASA GSFC and the National Imagery and Mapping Agency (NIMA) geopotential model EGM96*. NASA technical report NASA/TP-1998-206861. Available at: http://cddis.nasa.gov/926/egm96/egm96.html.

Maestro, A., Somoza, L., Rey, J., Martínez-Frías, J. & López-Martínez, J. 2007. Active tectonics, fault patterns, and stress field of Deception Island: a response to oblique convergence between the Pacific and Antarctic plates. *Journal of South American Earth Sciences*, **23**, 253–268.

Martín-Furones, A. 2000. *Análisis y ajuste de modelos de geoide. Observación y cálculo de la red gravimétrica de tercer orden en la Provincia de Valencia*. PhD thesis, Universidad Politécnica de Valencia, 163 pp..

Martí, J., Vila, J. & Rey, J. 1996. Deception Island (Bransfield Strait, Antarctica); an example of a volcanic caldera developed by extensional tectonics. *Geological Society Special Publication*, No. **110**, 253–265.

Mayer-Guerr, T., Zehentner, N., Klinger, B. & Kvas, A. 2014. *The satellite-only gravity field model ITSG-GRACE2014s*. Graz: Institute of Theoretical Geodesy and Satellite Geodesy, Graz University of Technology, Available at: http://itsg.tugraz.at/research/ITSG-Grace2014.

Pail, R., Goiginger, H., Schuh, W.-D., Höck, E., Brockmann, J.M., Fecher, T., Gruber, T., Mayer-Gürr, T., Kusche, J., Jäggi, A. & Rieser, D. 2010. Combined satellite gravity field model GOCO01S derived from GOCE and GRACE. *Geophysical Research Letters*, **37**, 10.1029/2010GL044906.

Pavlis, N.K., Holmes, S.A., Kenyon, S.C. & Factor, J.K. 2012. The development and evaluation of the Earth Gravitational Model 2008 (EGM2008). *Journal of Geophysical Research - Solid Earth*, **117**, 10.1029/2011JB008916.

Prates, G., Berrocoso, M., Fernández-Ros, A. & García, A. 2013. Enhancement of sub-daily positioning solutions for surface deformation monitoring at Deception volcano (South Shetland Islands, Antarctica). *Bulletin of Volcanology*, **75**, 10.1007/s00445-013-0688-3.

Reyes, R.B., Nagai, M., Kamiya, Y., Tipdecho, T. & Ninsawat, S. 2015. Effect of sea level rise in the validation of geopotential/geoid models in Metro Manila, Philippines. *Survey Review*, **47**, 211–219.

Seeber, G. 2003. *Satellite geodesy*, 2nd ed. Berlin: Gruyter, 589 pp.

Smellie, J.L. 2001. Lithostratigraphy and volcanic evolution of Deception Island, South Shetland Islands. *Antarctic Science*, **13**, 188–209.

Smellie, J.L. 2002. The 1969 subglacial eruption on Deception Island (Antarctica): events and processes during an eruption beneath a thin glacier and implications for volcanic hazards. *Special Publication of the Geological Society of London*, No. 202, 59–79.

Smellie, J.L., López-Martínez, J., Thomson, J.W. & Thomson, M.R.A. 2002. *Geology and geomorphology of Deception Island*. BAS GEOMAP Series, Sheets 6-A and 6-B, 1:25 000, supplementary text. Cambridge: British Antarctic Survey, 77 pp.

Torrecillas, C., Berrocoso, M. & Garcia, A. 2006. The Multidisciplinary Scientific Information Support System (SIMAC) for Deception Island, Antarctica. *In* Fütterer, D.K., Damaske, D., Kleinschmidt, G., Miller, H. & Tessensohn, F., *eds*. *Antarctica: contributions to global earth sciences*. Berlin: Springer, 397–402.

Torrecillas, C., Berrocoso, M., Perez-Lopez, R. & Torrecillas, M.D. 2011. Determination of volumetric variations and coastal changes due to historical volcanic eruptions using historical maps and remote-sensing at Deception Island (West Antarctica). *Geomorphology*, **136**, 6–14.

Valencio, D.A., Mendía, J.E., Vilas, J.F. 1979. Paleomagnetism and K-Ar age of Mesozoic and Cenozoic igneous rocks from Antarctica. *Earth and Planetary Science Letters*, **45**, 61–68.

Vidal, J., Berrocoso, M. & Fernández-Ros, A. 2012. Study of tides and sea levels at Deception and Livingston islands, Antarctica. *Antarctic Science*, **24**, 193–201.